Supporting Information

Carbon Nanothreads Enable Remarkable Enhancement in the Thermal Conductivity of Polyethylene

Haifei Zhan[1,2,*], Ying Zhou[2,3], Gang Zhang[4,*], Jihong Zhu[3], Weihong Zhang[3], Chaofeng Lü[1], and Yuantong Gu[2,*]

[1]*Department of Civil Engineering, Zhejiang University, Hangzhou 310058, P.R. China*

[2]*School of Mechanical, Medical and Process Engineering, Queensland University of Technology (QUT), Brisbane QLD 4001, Australia*

[3]*State IJR Centre of Aerospace Design and Additive Manufacturing, Northwestern Polytechnical University, Xi'an, Shaanxi 710025, China*

[4]*Institute of High Performance Computing, Agency for Science, Technology and Research, 1 Fusionopolis Way, Singapore 138632, Singapore*

***Corresponding Authors:**

Dr Haifei Zhan

Department of Civil Engineering, Zhejiang University, Hangzhou 310058, P.R. China, zhan_haifei@zju.edu.cn, +61 7 3138 1956

Professor Gang Zhang

Institute of High Performance Computing, A*STAR, 1 Fusionopolis Way, Singapore, 138632, zhangg@ihpc.a-star.edu.sg, +65 6419 1583

Professor Yuantong Gu

School of Mechanical, Medical and Process Engineering, Queensland University of Technology (QUT), Brisbane, QLD 4001, Australia, yuantong.gu@qut.edu.au, +61 7 3138 1009

S1. Contact surface calculation

For the PCFF force field, the Lenard-Jones potential between H atoms reaches the minimum value at the separate distance of σ = 2.995 Å, and the equilibrium distance between adjacent H atoms equals to d_{eq}^{HH} = 3.362 Å. Thus, compared to the isolated scenario, the maximum distance between the H atoms in the polymer matrix and the central axis of the NTH is $r_{max} = r_{NTH} + d_{eq}^{HH}$. Here, the equivalent radius of NTH is about 5 Å. Since the equivalent axial distance between adjacent NTHs is d_a = 6.25 Å,[1] each NTH can be approximated as a cylinder with a diameter between 6.25 Å and 11.72 Å. To estimate the effective interfacial surface area, an equivalent vdW diameter of $D_{vdW} = 7$ Å is adopted for the NTH embedded in the polymer matrix, as schematically illustrated in **Figure S1**. Take Case II for example, the interfacial surface area can be calculated from $S_{II} = 12LD_{vdW}(\pi - \theta)$, with L as the sample length and $\theta = \text{acos}\left(\frac{d_a}{D_{vdW}}\right)$. Its relative interfacial surface area (in relative to the evenly distributed pattern – Case I) can be defined as $\eta_S^{II} = \frac{S_{II}}{S_I} = 1 - \theta/\pi$. To note that using different equivalent vdW diameter will affect the magnitude of the relative interfacial surface area, while it will not change its relative changing trend and the conclusions.

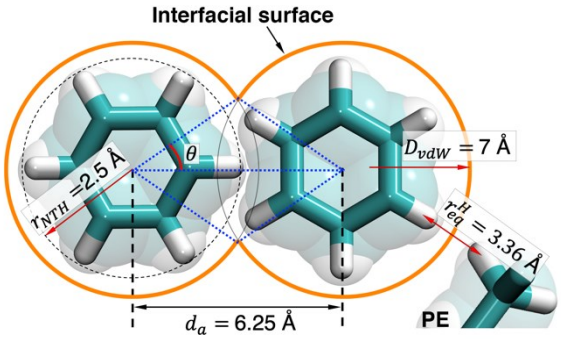

Figure S1 | Schematic view of the interfacial surface area calculation for two adjacent NTH fillers in the PE matrix.

S2. Heat transport for NTH wrapped by CNT

To investigate the heat transport of NTH under different interfacial environment, a model with an individual NTH wrapped by a single-walled CNT is adopted. As shown in **Figure S2**a, the (10,10) CNT was adopted as it provides a distance of around 0.3 nm (i.e., the graphite interlayer distance) between the CNT wall and the surface H atoms of the NTH. The NTH has a length of 12 nm. During the simulation, 0.5 nm in each end was fixed, and 1 nm in each end was selected as the heat source and sink, respectively. In the meanwhile, the CNT was treated as a rigid body to mimic a virtual wall and different Lenard-Jones (LJ) potential parameters were adopted to describe the interaction between the virtual wall and the NTH. The C-C interactions within the CNT were described by the modified Tersoff potential,[2] and the C-C and C-H interactions within the NTH were described by the AIREBO potential.[3-4] Figure S2b shows the heat flux in the cold and hot regions, which are highly consistent with each other, indicating a stable simulation. Specifically, the magnitude of the heat transferred in the NTH with a weaker H virtual wall exhibits a larger heat flux compared with the scenario with a stronger C virtual wall. Given the same simulation settings with a temperature drop of 20 K between the cold and hot regions, these results suggest a stronger interfacial interaction will suppress the thermal conductivity of NTH.

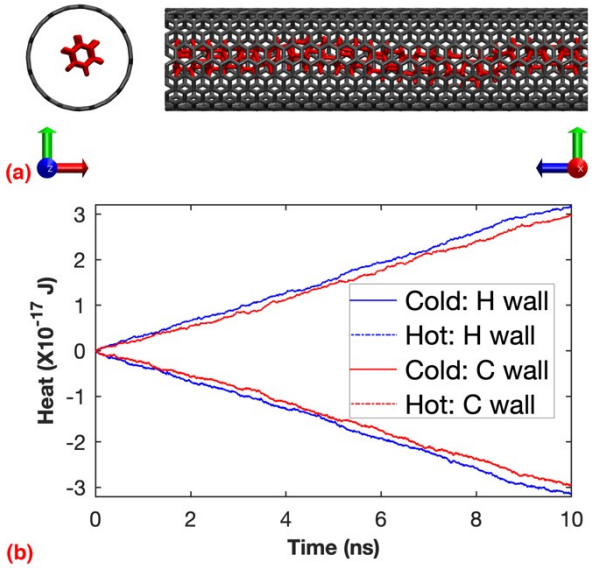

Figure S2 | (a) Schematic show of the NTH wrapped by (10,10) CNT; and (b) Time trajectory of the heat transferred in the NTH with a virtual H and C wall.

S3. Thermal transport properties of ethyl functionalized NTHs

Figure S3 compares the heat flux trajectory of the NTH without and with ethyl functions. As it is seen, the heat flux in the cold and hot regions are highly consistent with each other, indicating a stable simulation. Specifically, the magnitude of the heat transferred in the pristine NTH is nearly overlapped with that in the ethyl functionalized NTH. Given the same simulation settings with a temperature drop of 20 K between the cold and hot regions, these results suggest a similar thermal conductivity. Here, a short NTH with a length of about 12 nm is considered. Approximating the diameter as 0.5 nm, the thermal conductivity of the pristine and functionalized NTH is around 9 W/mK, which agrees well with our previous work.[5]

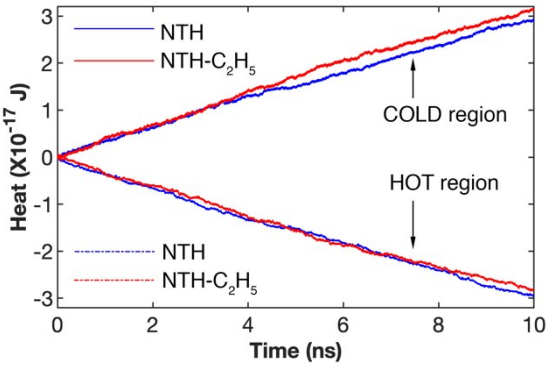

Figure S3 | Time trajectory of the heat transferred in the pristine NTH and (13.69%) ethyl functionalized NTH.

S4. Comparisons of the thermal transport properties between the samples with and without functional groups

It is obvious from **Figure S4a** that the sample with pristine NTH transfers more heat from the hot to the cold region, i.e., the sample without functional group possesses a higher thermal conductivity. The slightly higher thermal conductivity for the case with a low content of functional group (shown in Figure 4b main text) is basically due to the calculation errors as caused by the thermal fluctuations. Recall the definition, thermal conductivity is calculated from $\kappa = -J/\nabla T$, and there are inevitable numerical errors for the estimation of the temperature gradient ∇T and heat flux J. As demonstrated in Figure S4b, the extracted temperature value fluctuations, which leads to fitting errors for ∇T.

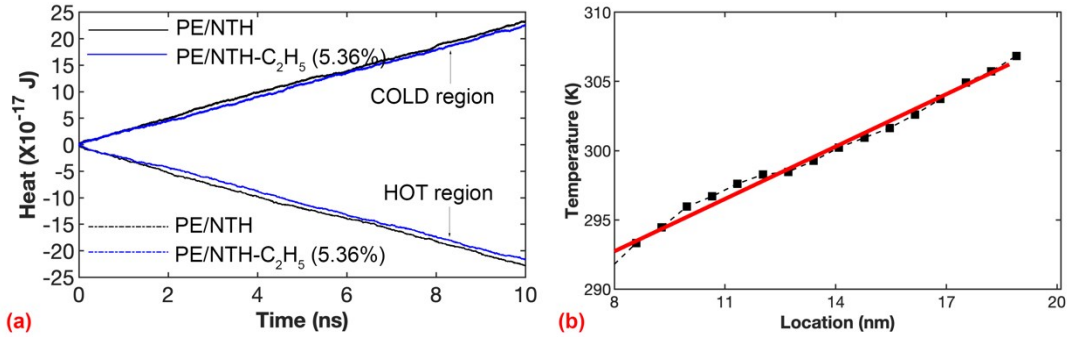

Figure S4 | Heat transfer for the samples with and without functional groups. (a)Time trajectory of the heat transferred for the sample with pristine NTH and (5.36%) ethyl functionalized NTH. (b) The temperature profile of sample with (5.36%) ethyl functionalized NTH at 4 ns. The dotted line with rectangular marker represents MD results, and the red solid line is the linear fitting.

S5. Atomic configurations at the NTH-C2H5/PE interface

Figure S5 shows the atomic configuration at the NTH/PE interface where the NTH contains 13.69% ethyl functionalization. As it is seen, large voids remain existing in the intermediate region during the whole simulation process.

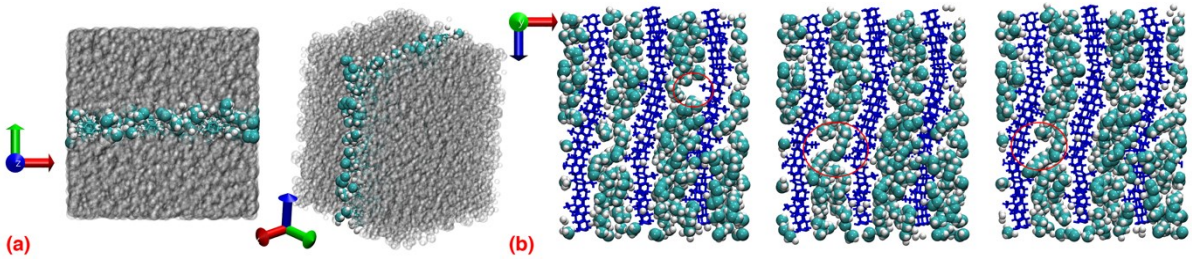

Figure S5 | The middle portion of the NTH-C2H5(13.69%) functionalized PE model showing the atomic configuration between adjacent NTHs. (a) The cross-sectional view (left panel) and the diagonal view (right panel) at the simulation time of 14.0 ns; and (d) The middle portion of the model showing the atomic configuration between adjacent NTHs at the simulation time of 14.5, 15.0, and 15.5 ns. The grey regions in a are hidden in b, and the red circles highlight the presences of voids.

S6. Vibrational density of states

Figure S6 shows the vibrational density of states (VDOS) for the polymer matrix and the NTH fillers. The PE nanocomposite with 12 evenly distributed NTH fillers is selected for the VDOS calculation. During the calculation, only the middle portion of the sample with a length of 50 Å is selected.

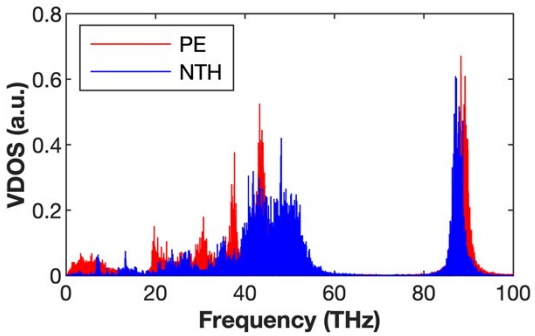

Figure S6 | Vibrational density of states (VDOS) for the polymer matrix and the NTH fillers.

References

[1] H. Zhan, G. Zhang, V. B. C. Tan, Y. Gu, Nature Communications 2017, 8, 14863.
[2] L. Lindsay, D. A. Broido, Physical Review B 2010, 81, 205441.
[3] D. W. Brenner, O. A. Shenderova, J. A. Harrison, S. J. Stuart, B. Ni, S. B. Sinnott, Journal of Physics: Condensed Matter 2002, 14, 783.
[4] S. J. Stuart, A. B. Tutein, J. A. Harrison, The Journal of Chemical Physics 2000, 112, 6472.
[5] H. Zhan, G. Zhang, Y. Zhang, V. B. C. Tan, J. M. Bell, Y. Gu, Carbon 2016, 98, 232.